

2-1-2008

Dynamical Transition in Sliding Charge-Density Waves with Quenched Disorder

Lee-Wen Chen
Syracuse University

Leon Balents
University of California - Santa Barbara

Matthew P. A. Fisher
University of California - Santa Barbara

M. Cristina Marchetti
Syracuse University, mcm@physics.syr.edu

Follow this and additional works at: <http://surface.syr.edu/phy>

 Part of the [Physics Commons](#)

Repository Citation

arXiv:cond-mat/9605007v1

This Article is brought to you for free and open access by the College of Arts and Sciences at SURFACE. It has been accepted for inclusion in Physics by an authorized administrator of SURFACE. For more information, please contact surface@syr.edu.

Dynamical Transition in Sliding Charge-density Waves with Quenched Disorder

Lee-Wen Chen⁽¹⁾, Leon Balents⁽²⁾, Matthew P. A. Fisher⁽²⁾
and M. Cristina Marchetti⁽¹⁾

⁽¹⁾ *Department of Physics, Syracuse University*

⁽²⁾ *Institute for Theoretical Physics, University of California, Santa Barbara*

(February 1, 2008)

We have studied numerically the dynamics of sliding charge-density waves (CDWs) in the presence of impurities in $d=1,2$. The model considered exhibits a first order dynamical transition at a critical driving force F_c between “rough” (disorder dominated) ($F < F_c$) and “flat” ($F > F_c$) sliding phases where disorder is washed out by the external drive. The effective model for the sliding CDWs in the presence of impurities can be mapped onto that of a magnetic flux line pinned by columnar defects and tilted by an applied field. The dynamical transition of sliding CDWs corresponds to the transverse Meissner effect of the tilted flux line.

PACS numbers: 71.45.Lr, 72.70.+m, 74.60.Ge

I. INTRODUCTION

The study of the dynamics of an ordered medium driven by an external force through quenched impurities is relevant to many physical systems. Examples include charge-density waves (CDWs) in anisotropic metals [1] and flux-line lattices (FLL) in the mixed state of type-II superconductors [2]. It has been argued that in both these systems impurities destroy the equilibrium long-range translational order (LRTO) and pin the medium. A driving force F , originating from an electric field or a current, can overcome the constraining forces from the impurities and cause the medium to slide. At $T = 0$, classical CDWs exhibit a depinning transition at a critical driving force F_T from a pinned ($F < F_T$) to a sliding ($F > F_T$) state. This transition has been described as a dynamic critical phenomenon. The nonlinear dynamics of the system near the critical point has been studied extensively both by numerical simulation [3] and by $4 - \epsilon$ expansions [4] and is fairly well understood.

In contrast, the dynamics of driven disordered media at large driving force, well above the depinning transition, has only recently begun to receive some attention. In the sliding state the pinning by impurities is less effective and it has been suggested that the medium may recover the LRTO at sufficiently large velocity. Recent experiments in YBCO as well as simulations of two-dimensional flux lattices have indeed shown that the flux array orders at large drives. Koshelev and Vinokur [5] have described this phenomenon as a true phase transition from a flowing liquid to a moving solid. Whether the ordering of driven flux lattices is a true dynamical phase transition or a crossover is still an open question.

Some of us recently addressed this class of questions by focusing on a model of driven CDWs in the presence of disorder and thermal noise [6]. The model considered in Ref. [6] allows for disorder-induced phase slips of the CDW. In three dimensions it yields a dynamical phase transition of the sliding CDW from a disordered phase with plastic flow to a temporally periodic “moving solid”

phase with quasi-long-range translational order. In two dimensions the moving solid phase is unstable due to the proliferation of phase slips.

In the present paper we focus on a related model of the dynamics of sliding CDWs that incorporates a nonequilibrium nonlinear term of the Kardar-Parisi-Zhang (KPZ) form [9], that was neglected in Ref. [6]. To render the analysis tractable with this addition, we have, however, neglected phase slips, and, for most of what follows, thermal fluctuations. While the neglect of thermal noise has very little effect upon our results, the omission of phase slips appears more severe. Indeed, the model considered here is by definition an elastic continuum at all driving forces and a “liquid phase” with dislocations cannot occur. We expect that at sufficiently low temperature and large driving force the omitted defects will make only minor changes to our results, at least on experimentally observable time scales. The true (infinite time) asymptotics is, however, likely to be affected by this omission.

Interestingly, despite its strong topological constraints, our model nevertheless exhibits a phase transition at a critical driving force F_c from an isotropic rough (disorder dominated) flowing phase at small driving forces, to an anisotropic smooth flowing phase where nonlinearities are washed out by the external drive. The average CDW velocity changes sharply at the transition, which is argued to be first order. The two phases are characterized by different values of the roughening exponent governing the growth of spatial fluctuations of the CDW phase with the size L_x of the system in the direction of the external drive (x -direction). In the rough phase the phase fluctuations grow linearly with L_x , $w(L_x, L_\perp) \sim L_x$, indicating that the elastic model breaks down. This suggests that in a corresponding model that allows for phase slips, this phase would be a flowing liquid. Above F_c the disorder is washed out in the direction of motion. Fluctuations are strongly suppressed in this direction and $w(L_x, L_\perp) \sim L_x^{1/2}$ for $L_x^z \gg L_\perp$, with $z \approx 0.85 \pm 0.05$.

Our results have two implications for CDW experi-

ments at high velocities, provided phase slip effects are sufficiently suppressed at low temperatures. First, above the critical force ($F > F_c$), translational correlations are expected to be highly anisotropic, decaying much more rapidly transverse to the motion than along it. This implies a substantial increase in the ratio of widths of Bragg scattering peaks,

$$\frac{d}{dF} \left(\frac{\Delta k_{\perp}}{\Delta k_{\parallel}} \right) > 0, \quad (1.1)$$

where Δk_{\perp} and Δk_{\parallel} are peak widths perpendicular and parallel to the CDW wave vector, respectively. Secondly, within our model, the non-equilibrium ordering transition is characterized by a jump discontinuity in the differential conductance $G_{\text{diff}} \equiv dI/dV$. As discussed in further detail in the next section, we are able to predict only the singular behavior of G_{diff} , and not the full non-linear form of the $I(V)$ curve.

We expect these two results to survive in varying degrees in models including phase slips (and hence experiments). The strong anisotropy of the translational correlations in the high-velocity phase should remain at low temperatures. The resistance singularity is expected to be more sensitive to phase slips (as, indeed, is the entire small F phase). Their effects are expected to round the step in G_{diff} very near to F_c .

II. EFFECTIVE MODEL FOR SLIDING CDWS

Charge-density waves are coupled electron-phonon excitations which exist in a class of anisotropic metals consisting of weakly coupled chains. In these materials the electronic density is sinusoidally modulated along the chain (x -) direction,

$$\rho(\mathbf{r}) = \rho_0 + \rho_1 \cos(2k_F x + \phi(\mathbf{r}, t)), \quad (2.1)$$

where k_F is the in-chain Fermi wave vector and ρ_1 the amplitude of the charge modulation. At low temperature, due to the gap in the dispersion relation for the amplitude, amplitude fluctuations are strongly suppressed and the dynamics can be described in terms of the phase ϕ only. The Hamiltonian \mathcal{H} for a CDW in a d -dimensional metal can be written as [1]

$$\begin{aligned} \mathcal{H} = & \frac{K}{2} \int d\mathbf{r} [(\nabla\phi)^2] \\ & + \int d\mathbf{r} V(\mathbf{r}) \rho_1 \cos(2k_F x + \phi(\mathbf{r}, t)), \end{aligned} \quad (2.2)$$

where we have rescaled coordinates to obtain an isotropic elastic term. The coefficient K is a stiffness constant. The effect of impurities is described via a Gaussian random potential $V(\mathbf{r})$ with zero mean, $\langle V(\mathbf{r}) \rangle = 0$, and short range correlations, $\langle V(\mathbf{r})V(\mathbf{0}) \rangle = V_0^2 \Delta(|\mathbf{r}|/\xi_0)$,

with ξ_0 a short wavelength cutoff. The overdamped equation of motion for the CDW phase variable ϕ is given by [10],

$$\begin{aligned} \partial_t \phi &= -\frac{D}{K} \frac{\delta \mathcal{H}}{\delta \phi} + \omega_0 \\ &= D \nabla^2 \phi + \omega_0 + \tilde{V}(\mathbf{r}) \sin(2k_F x + \phi(\mathbf{r}, t)), \end{aligned} \quad (2.3)$$

where $D = (\frac{m}{m^*})\tau v_F^2$ has the dimension of a diffusion constant ($l^2 t^{-1}$). Here τ is the relaxation time of a thermally excited phonon, while m and m^* are the electronic mass and effective mass, respectively. We have also let $\tilde{V}(\mathbf{r}) = (D/K)V(\mathbf{r})$. The second term on the right hand side of Eq. (2.3) arises from an electric field E applied along the x -direction, with $\omega_0 = Ee(\frac{\tau}{m^*})2k_F$, and can be shifted away by $\phi \rightarrow \phi + \omega_0 t$. The “force” ω_0 has dimensions of frequency (t^{-1}) and actually represents the “washboard frequency” $\omega_0 = 2k_F v$ of a freely sliding CDW (with velocity v) driven by an external electric field E , in the absence of quenched disorder. Equation (2.3) is the conventional Fukuyama-Lee-Rice (FLR) model of CDW dynamics [10], which has been studied extensively both analytically and numerically, particularly near the depinning transition. The FLR model exhibits a depinning transition at a threshold field E_T , corresponding to a threshold force $\sigma_T = E_T e(\frac{\tau}{m^*})$.

As discussed in Ref. [6], the FLR equation is incomplete in the strongly driven regime. It is essentially a near-equilibrium description, in which only the most relevant perturbation (the driving field) has been added to the equilibrium relaxational dynamics. Several additional effects become important in the sliding state.

The most important such effect is that of *convection*. In particular, in a CDW moving with velocity v , the partial time derivative ∂_t in Eq. 2.3 must be replaced by the total convective derivative $D_t = \partial_t + v\partial_x$. More generally, the linear derivative ($\partial_x \phi$) term arises because the electric field breaks the reflection symmetry $x \rightarrow -x$. Note that the coefficient of this term is small for small velocities, which is why it is neglected in the usual equilibrium and near-static (i.e. CDW depinning) contexts.

A second term ordinarily omitted from the FLR equation in equilibrium arises from coupling to the underlying periodic lattice. This intrinsic pinning in the direction of motion can be incorporated in Eq. (2.3) by the replacement $V(\mathbf{r}) \rightarrow V(\mathbf{r}) + W(x)$, where $W(x)$ is a periodic potential, $W(x) = W_0 \cos(Qx)$, and Q is in general incommensurate with $2k_F$. While in other contexts such an incommensurate periodic potential can be safely neglected, we will see that it gives rise to important effects for the asymptotic behavior in the strongly driven limit.

Including both these effects, we arrive at a suitable generalization of the FLR equation,

$$\begin{aligned} \partial_t \phi &= D \nabla^2 \phi + \omega_0 - \sigma \partial_x \phi \\ &+ [\tilde{V}(\mathbf{r}) + \tilde{W}(x)] \sin(2k_F x + \phi(\mathbf{r}, t)), \end{aligned} \quad (2.4)$$

where again a numerical factor has been absorbed into the periodic potential $\tilde{W}(x)$. We have allowed for renor-

malizations of the convective term by keeping the coefficient σ general, but we expect $\sigma \sim v$. Eq. 2.4 is capable of describing the behavior of the CDW (up to the aforementioned caveats respecting phase slips and thermal fluctuations) in the full range of applied fields from well below to far above the nominal threshold field.

In fact, Eq. 2.4 is so general that it is a rather inappropriate point from which to study the moving state. This is made evident by making the transformation $\phi = \omega_0 t + \tilde{\phi}$, in order to focus on the fluctuations $\tilde{\phi}$ around the uniformly sliding CDW. The resulting equation of motion for $\tilde{\phi}$ contains force terms which oscillate rapidly in time. To determine their effect at time scales longer than $2\pi/\omega_0$, one must develop instead an *effective* equation of motion for a coarse-grained (temporally and spatially averaged) phase $\bar{\tilde{\phi}}$. In what follows we will drop the overbar and denote the coarse-grained phase variations simply by $\tilde{\phi}$.

The coarse-graining procedure may be explicitly performed in two different ways. The simplest method is a variant of the high-velocity expansion about the sliding state [7], obtained by iterating a formulation of Eq. 2.4 as an integral equation. A more complicated, but conceptually more clear approach is to coarse-grain using renormalization group (RG) methods, in which short wavelength and high frequency components of $\tilde{\phi}$ are explicitly integrated out in a field-theoretic formulation. A similar calculation was carried out recently in a different context by Rost and Spohn [12]. Both approaches are straightforward but tedious, and we simply quote the results in what follows [8].

Several simplifications are obtained in this effective coarse-grained description. The most important is the modification of the random potential term $\tilde{V}(\mathbf{r}) \sin(2k_F x + \phi)$, which, as mentioned before becomes oscillatory. A careful treatment reveals, however, that this term does not strictly average to zero in the coarse-grained model. Instead, as discussed in Refs. [11,6], it generates an effective spatially varying drag force $F_p(\mathbf{r})$. To leading order in $\frac{1}{\omega_0}$, its correlations are $\langle F_p(\mathbf{r}) F_p(\mathbf{0}) \rangle = F_0^2 \delta(\mathbf{r})$ with $F_0 = \frac{\tilde{V}_0^2}{4\omega_0}$. This may be understood physically as simply reflecting variations of the impurity density in different regions of the sample, which then exert a spatially random drag force on the CDW.

An important difference between this term and the original sine-Gordon type term is that it does not prefer any particular value of the phase variation $\tilde{\phi}$. This is in fact an exact result in the moving phase, reflecting the non-trivial transformation property $\phi \rightarrow \phi + \omega_0 \tau$ under a time-translation $t \rightarrow t + \tau$. In general terms, the equilibrium ordered phase of the CDW is described as a state of spontaneously broken spatial translation symmetry. This state is highly susceptible to disorder, because randomness explicitly breaks precisely this symmetry – i.e. it acts as a random field. By contrast, the sliding CDW breaks *time*-translation symmetry, which is an ex-

act invariance of the system, even with $\tilde{V} \neq 0$.

A second simplification occurs in the intrinsic pinning term. Like the random potential, this term also becomes oscillatory in time, but generates a non-trivial correction upon coarse-graining. To second order in a gradient expansion, the correction has the form of an additional drag force $\delta F_W \sim -\frac{W_0^2}{2\omega_0} [1 - c_1 |\nabla_\perp \tilde{\phi}|^2 - c_2 |\partial_x \tilde{\phi}|^2]$, where $c_1 \sim c_2 \sim 1/(2k_F)^2$ are constants. Physically, the gradient corrections arise because the drag force from intrinsic pinning becomes less effective as the CDW wavevector (whose local shift is proportional to $\nabla \tilde{\phi}$) becomes less commensurate with the underlying lattice. For simplicity, we will focus on the isotropic case $c_1 = c_2$, which is expected to be approximately correct for CDWs whose density profile is well approximated by the single Fourier harmonic form of Eq. 2.1 and which is not too far from commensurability. The resulting gradient-squared correction is a realization of the Kardar-Parisi-Zhang (KPZ) nonlinearity in the CDW system.

The final coarse-grained equation of motion is

$$\partial_t \tilde{\phi} = D \nabla^2 \tilde{\phi} - \sigma \partial_x \tilde{\phi} + F_p(\mathbf{r}) + \frac{\lambda_0}{2} (\nabla \tilde{\phi})^2, \quad (2.5)$$

where $\lambda_0 \sim \frac{W_0^2}{(8\omega_0 k_F^2)}$. This coefficient is positive, because a mis-oriented CDW (with $\nabla \tilde{\phi} \neq 0$) is less slowed down than an aligned one (with $\nabla \tilde{\phi} = 0$).

Eq. 2.5 is the basis for our study of the moving state. We caution, however, that some information is lost in this approach, and various non-universal high energy features of the CDW behavior are no longer easily calculable. An important example is the full form of the I-V curve. As can be explicitly seen in the coarse-graining procedure, the CDW frequency $\partial_t \phi$ as a function of E or ω_0 has non-trivial contributions from the short-wavelength degrees of freedom not contained in Eq. 2.5. An additional difficulty is that the drag forces F_0 and λ_0 are strongly force dependent. Our long-wavelength description *does*, however, capture the *singular* part of the CDW velocity. We define

$$\delta v_{sing} = \overline{\langle \partial_t \tilde{\phi} \rangle}, \quad (2.6)$$

where the overbar denotes a spatial average and the brackets denote the disorder average. The quantity δv_{sing} is actually a frequency shift. Note that, because this includes only the singular part of the $v(\omega_0)$ relation, there is no particular preferred sign for $d\delta v_{sing}/d\omega_0$.

The spatial fluctuations of the phase can be characterized by their growth with the system size. A useful measure of such fluctuations employed in the study of interface dynamics is the "interface width" in the long-time saturated regime, given by

$$w(L_x, L_\perp) \equiv \overline{\langle [\phi(\mathbf{r}, t) - \overline{\phi(\mathbf{r}, t)}]^2 \rangle}^{1/2} \quad (2.7)$$

in a d-dimensional system of size $L_x L_\perp^{d-1}$.

If the KPZ term is neglected in Eq. (2.5), the equation is linear and can be solved exactly by Fourier transformation, as discussed in Ref. [6]. The CDW response is linear and $\langle \overline{\partial_t \phi} \rangle = \omega_0$, i.e., $\delta v_{sing} = 0$. The random mobility yields a static distortion of the CDW,

$$\tilde{\phi}(\mathbf{q}, \omega) = \frac{F_p(\mathbf{q})}{Dq^2 + i\sigma q_x} 2\pi\delta(\omega). \quad (2.8)$$

The corresponding correlation function is $\langle |\tilde{\phi}(\mathbf{q}, \omega)|^2 \rangle = S(q)2\pi\delta(\omega)$, with $S(q) = \frac{F_0^2}{(Dq^2)^2 + \sigma^2 q_x^2}$ the static structure function. The $\sigma\partial_x\phi$ term in Eq. (2.5) is crucial in determining the decay of spatial correlation in the moving state. If this term is absent, fluctuations are isotropic, with $S(q) \sim q^{-4}$, so that $w(L) \sim L^{(4-d)/2}$, for $L_x = L_\perp = L$. In particular in $d = 1$, $w(L) \sim L^{3/2}$ and the system will develop a ‘‘groove’’ instability of the type discussed in [13]. The case $d = 2$ is marginal with $w(L) \sim L$. The $\sigma\partial_x\phi$ term suppresses the growth of fluctuations in the x -direction. When this term is present, in the limit where $L_x \gg L_\perp$ and $\sigma \gg 1$, the CDW is ‘‘riding over’’ the static disorder and $w(L_x, L_\perp) \sim L_x^{1/2}$.

III. TILTED MAGNETIC FLUX LINE ANALOGY

When the KPZ coupling λ_0 is nonzero, Eq. (2.5) can be mapped into the problem of a directed path in a random potential via the well known Cole-Hopf transformation [14]. By letting $\Psi(\mathbf{r}, t) = e^{\frac{\lambda_0}{2D}\tilde{\phi}(\mathbf{r}, t)}$, a linear equation of motion for $\Psi(\mathbf{r}, t)$ is obtained,

$$\partial_t \Psi = [\sigma\partial_x + D\nabla^2 + \frac{\lambda_0}{2D}F_p(\mathbf{r})]\Psi. \quad (3.1)$$

The solution of Eq. (3.1) can be written as a path-integral,

$$\Psi(\mathbf{r}, t) = \int_{(\mathbf{0},0)}^{(\mathbf{r},t)} \mathcal{D}[\mathbf{r}] e^{-\frac{1}{2D} \int_0^t dt' [\frac{1}{2}(d\mathbf{r}/dt')^2 - \sigma\hat{x} - \lambda_0 F_p(\mathbf{r})]}. \quad (3.2)$$

Eq. (3.2) can also be interpreted as the partition function of a tilted magnetic flux line in the presence of columnar pinning centers. A single magnetic flux line in a $(d+1)$ -dimensional sample of thickness L in the direction of the applied field \mathbf{H} , chosen as the z direction ($\mathbf{H} = H_0\hat{\mathbf{z}}$), is parametrized by its trajectory $\mathbf{r}(z)$ as it traverses the sample along the field direction. The sample contains columnar pinning centers aligned with the z -direction that can pin the flux line over its entire length. An additional magnetic field \mathbf{H}_\perp applied perpendicular to the z -direction tilts the flux line away from the direction of the columnar pins. The flux line free energy is then given by,

$$G = \int_0^L dz \left\{ \frac{\tilde{\epsilon}_1}{2} \left[\frac{d\mathbf{r}}{dz} - \frac{\mathbf{h}}{\tilde{\epsilon}_1} \right]^2 + U(\mathbf{r}(z)) \right\}, \quad (3.3)$$

where $\tilde{\epsilon}_1 = (\frac{\phi_0}{4\pi\lambda_{ab}})^2 \ln(\kappa)$ is the tilt modulus (we assume for simplicity an isotropic superconductor), $\mathbf{h} = \mathbf{H}_\perp\phi_0/4\pi$, and $U(\mathbf{r})$ is the random pinning potential generated by the columnar defects. The pinning potential is correlated along the direction and has short range correlations in the plane, with $\langle U(\mathbf{r})U(\mathbf{r}') \rangle = \Delta\delta(\mathbf{r} - \mathbf{r}')$. The partition function of a vortex line with fixed end points $\mathbf{r}(0) = \mathbf{0}$ and $\mathbf{r}(L) = \mathbf{r}_\perp$ is obtained by summing the Boltzmann factor $e^{-G/k_B T}$ over all paths connecting the end points and it is given by

$$Z = \int_{(\mathbf{0},0)}^{(\mathbf{r},t)} \mathcal{D}[\mathbf{r}] e^{-\frac{1}{T} \int_0^L dz \left\{ \frac{\tilde{\epsilon}_1}{2} \left[\frac{d\mathbf{r}}{dz} - \frac{\mathbf{h}}{\tilde{\epsilon}_1} \right]^2 + U(\mathbf{r}(z)) \right\}}. \quad (3.4)$$

The dynamics of a d -dimensional driven CDW at $T = 0$ can therefore be mapped onto the tilt response of a magnetic flux line in a $(d+1)$ -dimensional superconductor with columnar pins, at finite temperature. In this mapping the time argument of the CDW corresponds to the flux line coordinate z along the field direction, the diffusion constant D plays the role of temperature, according to $D \rightarrow \frac{T}{2\tilde{\epsilon}_1}$, and the driving force σ corresponds to a tilt field $\mathbf{h} = h\hat{x}$ with $\sigma \rightarrow \frac{h}{\tilde{\epsilon}_1}$. The correspondence between the various CDW and flux line quantities is summarized in table 1.

CDW	Flux line
D	$T/2\tilde{\epsilon}_1$
σ	$h/\tilde{\epsilon}_1$
$\lambda_0 F_0$	$\sqrt{\Delta}/\tilde{\epsilon}_1$
$-\lambda_0\delta v_{sing}$	$g/\tilde{\epsilon}_1$
$\lambda_0 \frac{d\delta v_{sing}}{d\sigma}$	m_\perp

Table 1

Eqs. (3.4) and (3.2) differ by a constant term $\frac{h^2 L}{2\tilde{\epsilon}_1}$ in the flux line free energy which represents the field energy associated with the tilt field \mathbf{H}_\perp . In the absence of a tilt field, the flux line is localized on the strongest columnar defect. At low temperature the localization length, defined as the radius of the tube to which the flux line is confined, is of the order of the range of the pinning potential. Thermal fluctuations increase the localization length, but are not sufficient to depin the flux line in $d = 1, 2$. A sufficiently strong perpendicular field \mathbf{H}_\perp will, however, depin the flux line. The response of the flux line to the field is measured by the average induction in the direction B_\perp of the transverse field. We define a dimensionless induction $b_\perp = \frac{B_\perp}{n_0\phi_0}$. This is also the mean slope of the tilted flux line. The induction can be written

as $b_{\perp} = \frac{h}{\epsilon_1} + 4\pi m_{\perp}$, where $m_{\perp} = -\frac{\partial g}{\partial h}$ is the (dimensionless) total magnetization and $g(h)$ is the Gibbs free energy per unit length of the tilted flux line. It has been argued that a flux-line array pinned by columnar defects exhibits a transverse Meissner effect, with $b_{\perp} = 0$ for tilt field below a critical value h_c and $b_{\perp} \neq 0$ for $h > h_c$. The tilt response of a *single* flux line pinned by *one* columnar defect in $(1+1)$ -dimensions can be evaluated analytically (see Appendix A and [16]). One finds that in the limit $L_x \rightarrow \infty$ there is a transverse Meissner effect for $h < h_c$. For a δ -function pin with $U(\mathbf{r}) = -U_0\delta(\mathbf{r})$, we find $h_c = \frac{U_0}{T} \frac{4\pi\epsilon_1}{\phi_0}$. In the pinned configuration for $h < h_c$ the flux line free energy per unit length is $g = \frac{(h^2 - h_c^2)}{2\epsilon_1}$, so that $m_{\perp} = -\frac{h}{\epsilon_1}$ and $b_{\perp} = 0$. For $h \geq h_c$ the line is depinned and $g = 0$. This gives $m_{\perp} = 0$ and $b_{\perp} = \frac{h}{\epsilon_1}$. The transition from a pinned to a depinned configuration is associated with a jump discontinuity in the induction or tilt slope b_{\perp} at h_c and can therefore be classified as a *first order* phase transition. For a general pinning potential we estimate h_c as the field required to depin the flux line, $h_c^2/2\epsilon_1 \sim \sqrt{\Delta}$, or $h_c \sim (2\epsilon_1\sqrt{\Delta})^{1/2}$. Similar conclusions were reached by Balents and Simon [15] for the tilt response of a single flux line in a random distribution of columnar pins in $(1+1)$ -dimension. Also Hatano and Nelson [16] very recently related the depinning of a flux line from columnar defects by a transverse field to the localization transition of a quantum particle in a constant imaginary vector potential. By exploiting this mapping they showed that the transverse Meissner effect persists in both $d = 1, 2$. The question of whether an array of many *interacting* flux lines pinned by columnar defects will also exhibit a sharp transition is, however, still open.

The transverse Meissner effect for the vortex line translates into a *first order* dynamical phase transition of the sliding CDW. We recall that the CDW driving force σ corresponds to the tilt field h and $\delta v_{sing} \sim g$. There is then a transition at a characteristic σ_c from a state with $\delta v_{sing} \neq 0$ for $\sigma < \sigma_c$ to a state where the external drive dominates and washes out the effect of disorder in the direction of the drive, yielding $\delta v_{sing} = 0$ for $\sigma < \sigma_c$. The driving force σ_c where the transition occurs can be estimated from the flux-line analogy using table 1 and the estimated $h_c \approx (2\epsilon_1\sqrt{\Delta})^{1/2}$ as $\sigma_c \approx \sqrt{2\lambda_0 F_0}$. The sliding phase with $\delta v_{sing} \neq 0$ at small driving forces corresponds to the situation where the flux line is pinned on the strongest columnar defects and exhibits a transverse Meissner effect. As we will show in the next section, this is a disorder-dominated regime for the sliding CDW with a “rough” spatial profile of the phase $\phi(\mathbf{r}, t)$. We will refer to this phase as a rough sliding phase. For $\sigma \geq \sigma_c$ the CDW is in a sliding phase with $\delta v_{sing} = 0$, corresponding to a flux line depinned by the tilt field and “riding over” the columnar pins. As shown below, this phase is characterized by anisotropic spatial fluctuations of the phase. Fluctuations are suppressed in the direction of the

driving force and we will refer to this phase as a “flat” phase.

IV. NUMERICAL RESULTS

We have integrated numerically Eq. (2.5) in both $d = 1, 2$ by discretizing the spatial coordinates, with lattice spacing equal to the range R_p of the pinning potential, chosen as our unit of length. We assume an initially flat configuration, $\phi(\mathbf{r}, t = 0) = 0$, and follow the dynamics until the system relaxes to a steady state. The relaxation time scales as $L_x^2 L_{\perp}^{2d-2}$. The average CDW properties in the saturated sliding state are evaluated by performing both a time average and an average over many realizations of the disorder.

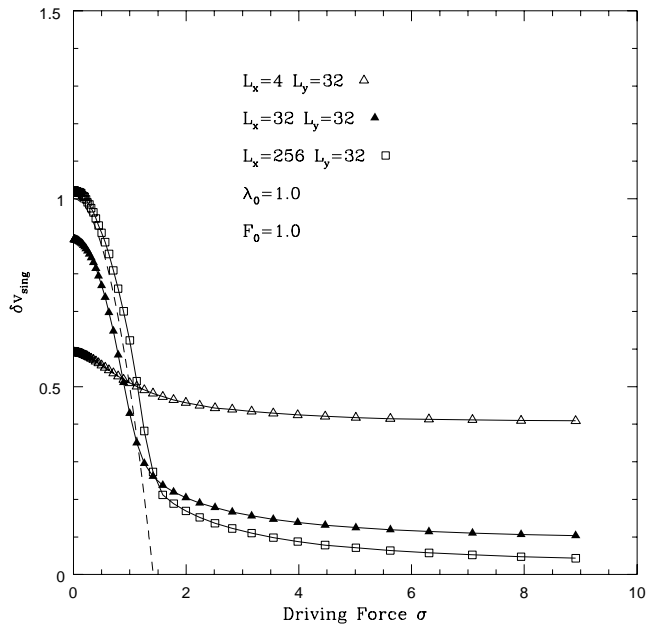


Fig.1

Figure 1 shows the frequency shift δv_{sing} of the CDW defined in Eq. (2.6) as a function of the driving force σ for $d = 2$. A similar behavior is obtained in $d = 1$. As the system size L_x is increased one observes a transition between two sliding phases. For the parameter values used here the estimated critical force is $\sigma_c = \sqrt{2}$, a value that agrees quite well with our numerical results. At large driving forces disorder is washed out by the external drive and δv_{sing} approaches zero as $L_x \rightarrow \infty$. For small driving forces both impurities and intrinsic pinning are important and yield a large δv_{sing} . While the drop of δv_{sing} above a critical force does become sharper as L_x increases, the approach to the sharp transition expected in the limit $L_x, L_{\perp} \rightarrow \infty$ is rather slow. This can be understood by examining the dependence on the system size L_x of the free energy of a single flux line pinned by a

single columnar defect evaluated in Appendix A. As discussed in the previous section, this simple model exhibits a first-order depinning transition in the limit $L_x \rightarrow \infty$. On the other hand, the finite size corrections to the flux line free energy are large in the region $h > h_c$, as shown in Fig. 5. For $h < h_c$ the flux line is localized on the columnar pin and does not “see” the rest of the system. As a result, in this region the finite size corrections to the free energy vanish exponentially with system size. For $h > h_c$ the flux line is delocalized and samples the entire system. In this region the free energy is quite sensitive to the finite system size, with $g(L_x) - g(\infty) \sim \frac{1}{L_x}$. The scaling of $\delta v_{sing}(L_x, L_\perp)$ in our driven CDW problem - which maps onto a tilted flux line pinned by a random distribution of *many* columnar defects - is even slower than obtained in the single pin model, with $\delta v_{sing} \sim L_x^{1/2}$ approximately. This slow approach to the asymptotic limit can, however, be understood by the same physical argument.

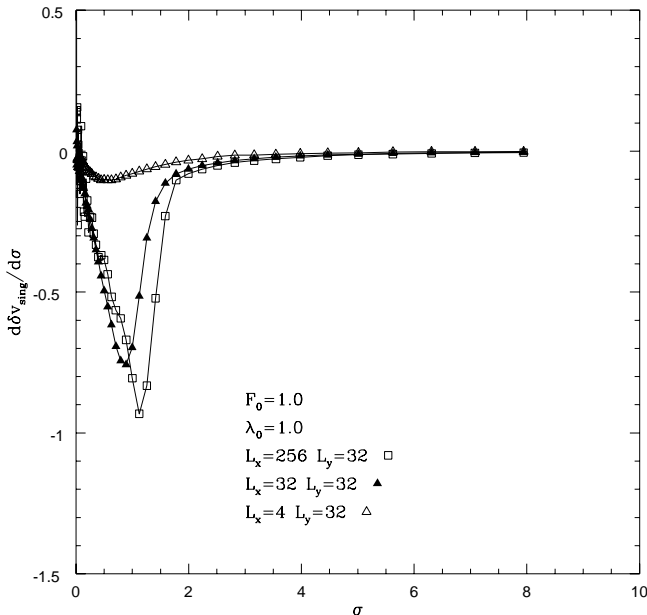


Fig.2

To better display the change of δv_{sing} at the transition we show in Fig. 2 the evolution of the curve $\frac{dv_{sing}}{d\sigma}$ versus σ with system size L_x for $d = 2$. In the limit $L_x \rightarrow \infty$ the derivative will exhibit a jump discontinuity at the transition. As the driving force σ is proportional to the applied voltage (electric field) and δv_{sing} is proportional to the current I , this corresponds to a jump discontinuity in the differential conductance $G_{diff} = \frac{dI}{dV}$. Our model only allows us to predict the singular shift δv_{sing} and therefore the singular behavior of G_{diff} , but not the full nonlinear form of the $I(V)$ curve. The magnitude of the jump discontinuity in $\frac{dv_{sing}}{d\sigma}$ is, however, proportional to the jump discontinuity in G_{diff} . The precise relation and

the possibility of observing this effect will be discussed in the next section. From table 1 we see that $\frac{dv_{sing}}{d\sigma}$ corresponds to the magnetization of the tilted flux line. Fig. 2 displays then the transverse Meissner effect discussed earlier.

By translating the results obtained in Appendix A for the flux line, we find that if the random force $F_p(\mathbf{r})$ of Eq. (3.1) is replaced by a single δ -function pin, the frequency δv_{sing} is given by

$$\delta v_{sing} = \frac{\sigma_c^2 - \sigma^2}{2\lambda_0}. \quad (4.1)$$

This form is shown as a dashed line in Fig.1 and fits very well our data for $\sigma < \sigma_c$. This is easily understood because in the region $\sigma < \sigma_c$ the flux line is localized onto the strongest pin and its free energy is basically unaffected by the presence of the other defects.

The two sliding states of the driven CDW differ qualitatively in the behavior of the spatial fluctuations of the coarsened-grained phase $\phi(\mathbf{r}, t)$. For $\sigma < \sigma_c$ pinning dominates the dynamics. The sliding state is rough with large spatial fluctuations of the phase both in the directions parallel and perpendicular to the external drive σ . For $\sigma > \sigma_c$ the term $\sigma \partial_x \phi$ washes out the effect of pinning in the x -direction, damping out phase fluctuations in this direction. In this case, the spatial fluctuations of the phase are anisotropic and are suppressed in the direction of the external drive. This behavior is shown qualitatively in Fig. 3 that displays contour plots of the CDW phase for increasing values of σ .

To quantify the behavior of phase fluctuations in the two sliding states, we have examined the interface width $w(L_x, L_\perp)$ defined in Eq. (2.7). In the isotropic disorder-dominated phase for $\sigma < \sigma_c$ we expect $w \sim L_x \sim L_\perp$. To understand this, we recall that when $\sigma = 0$ the path-integral solution (3.2) of the CDW problem can also be interpreted as the transfer matrix solution of the Schrödinger equation for a quantum particle in a random potential in d spatial dimensions and imaginary time [16]. The width $w(L_x, L_\perp)$ corresponds to the fluctuations in the energy of the quantum particle as a function of system size. For $d = 1$ the quantum particle is always localized. The states are exponentially localized and one can show [17] that the energy fluctuations scale as the system size, i.e., $w(L_x) \sim L_x$. A similar behavior is expected for $d = 2$. In the large- σ phase, we postulate an anisotropic scaling ansatz for the interface width,

$$w(L_x, L_\perp) = L_x^\chi f(L_\perp/L_x^z), \quad (4.2)$$

where χ and z are two new exponents. For $L_x^z \gg L_\perp$ the system looks one-dimensional, extended along the x -direction. An approximate equation of motion in this regime is obtained from Eq. (2.5) with $\nabla \rightarrow \partial_x$. For large σ both pinning by impurities and intrinsic pinning which yields the KPZ nonlinearity are negligible compared to the $\sigma \partial_x \phi$ term and one can obtain an approximate solution of the equation, which yields $w(L_x, L_\perp) \sim L_x^{1/2}$.

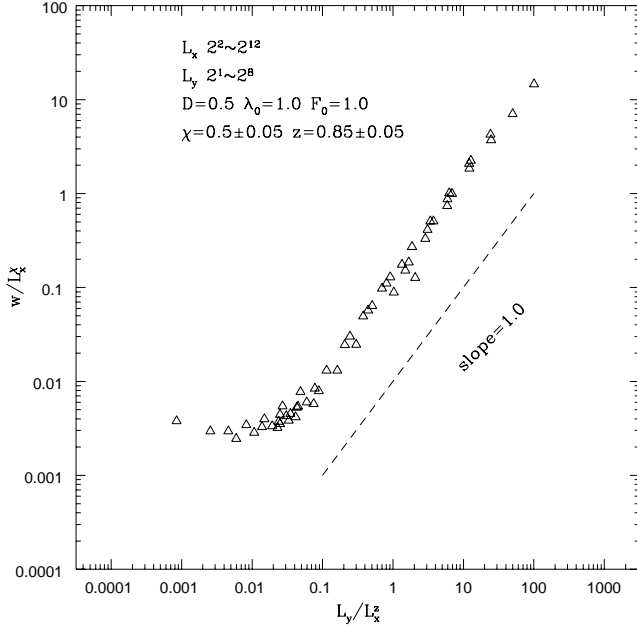


Fig.4

The scaling function $f(s)$ in Eq. (4.2) must therefore obey $f(s) \sim s^{\frac{x-1/2}{z}}$ for $s \ll 1$. This result is easily understood by exploiting the mapping of driven CDW dynamics onto the problem of the tilted magnetic flux line. For $\sigma \gg \sigma_c$ ($h \gg h_c$) the flux line is delocalized and “rides over” many columnar defects. The interface width $w(L_x, L_\perp)$ corresponds the fluctuations of the flux line free energy, which in this limit is determined by a sum of independent random energies, yielding a $w(L_x, L_\perp) \sim L_x^{1/2}$ scaling for $L_x^z \gg L_\perp$. In the opposite limit, $L_\perp \gg L_x^z$, the system looks one-dimensional along the y -direction for $d = 2$. The $\sigma \partial_x \phi$ term has no effect and fluctuations are dominated by disorder, with the result $w(L_x, L_\perp) \sim L_\perp$. This follows again from the exponential localization of states of a one-dimensional quantum particle in a random potential. The scaling function obeys $f(s) \sim s$ for $s \gg 1$ and $w(L_x, L_\perp) \sim L_x^{\chi-z} L_\perp$ for $L_\perp \gg L_x^z$ in $d = 2$. A scaling collapse of our numerical results for the interface width in $d = 2$ is shown in Fig. 4. The best collapse is achieved with $\chi = 0.5 \pm 0.05$ and $z = 0.85 \pm 0.05$. These results agree well with the asymptotic values discussed earlier.

V. CONCLUSION

We have studied the dynamics of driven CDWs moving through a random medium at zero temperature, at driving forces well above the threshold force where the depinning transition occurs. The CDW model considered incorporates new nonequilibrium terms which are important in the strongly driven regime and are gener-

ally not included in the FLR model. We have found that in $d = 1, 2$ the driven CDW exhibits a first order phase transition at a critical driving force $\sigma_c \sim \sqrt{2\lambda_0 F_0}$. For $\sigma < \sigma_c$ disorder controls the dynamics yielding a rough sliding phase with spatial fluctuations of the phase that grow linearly with L_x , indicating that the phase-only model breaks down. For $\sigma > \sigma_c$, the driving force washes out the effect of disorder in the direction of motion. The CDW slides uniformly with $\delta v_{sing} = 0$. This moving phase is highly anisotropic as the external drive suppresses the spatial fluctuations of the phase in this direction. The CDW remains “rough” in the direction transverse to the external drive. By using the Cole-Hopf transformation, the problem of CDW dynamics at large driving force can be mapped onto the problem of the tilt response of a magnetic flux-line pinned by columnar defects. The dynamical transition of the sliding CDW corresponds to the transverse Meissner effect of the tilted flux line.

Our coarsened-grained model of phase dynamics given in Eq. (2.5) only applies in the strongly driven phase, well above the $T = 0$ threshold field, E_T . In the weak pinning limit, one can relate E_T to the Lee-Rice length L_0 that represents the typical domain size in a pinned CDW. The pinning length L_0 is the length where the elastic strains induced by disorder are of order one and is given by $L_0 = \left[\frac{\hbar v_F \pi}{V_0} \left(\frac{\xi_0^{d/2}}{c^d - 1} \right) \right]^{\frac{2}{4-d}}$. Here c is the average spacing between the CDW chains and ξ_0 is the range of the disorder potential. We expect $\xi_0 \sim c$. The threshold field is then estimated by balancing the total force on a domain of size L_0 to the elastic force acting on the same domain, with the result, $E_T = \frac{\hbar v_F k_F}{2ec^d} L_0^{d-2}$. This corresponds to a threshold force $\sigma_T = E_T e (\frac{\tau}{m^*})$. The first order transition is predicted to occur at a critical force

$$\sigma_c \sim \sqrt{2\lambda_0 F_0}, \quad (5.1)$$

where to leading order in $\frac{1}{\sigma}$, $\lambda_0 \sim \frac{W_0^2}{8k_F^2 \sigma}$ and $F_0 \sim \frac{V_0^2}{4k_F \sigma}$. Recalling that $\sigma = Ee\tau/m^*$, we can solve Eq. (5.1) self-consistently for a critical field E_c , with the result

$$E_c = \left(e \frac{\tau}{m^*} \right)^{-1} \sigma_c = \left(\frac{\pi \rho_1}{e} \right) \sqrt{W_0 V_0}. \quad (5.2)$$

The first order transition will only be observable if $E_c \gg E_T$. We find $E_c/E_T \sim \frac{2\pi^2 \rho_1}{k_F} \sqrt{\frac{W_0}{V_0}} \left(\frac{\xi_0}{L_0} \right)$ for $d = 2$. The first order phase transition at E_c may therefore be observable in a dirty material ($L_0 \approx c$) with appreciable intrinsic pinning ($W_0 \gg V_0$). Using the results of our calculation of the tilt response of a flux line pinned by a single defect (Appendix A), we estimate the magnitude of the jump discontinuity in δv_{sing} at σ_c as $|\frac{dv_{sing}}{d\sigma}| \approx \frac{\sigma_c}{\lambda_0} = \sqrt{2F_0/\lambda_0}$. This corresponds to a jump discontinuity in G_{diff} that can be expressed in terms of microscopic CDW parameters as $\Delta G_{diff} = \left(\frac{k_F}{\pi c} \right) \left(\frac{L_\perp}{L_x} \right) \frac{2e^2 \tau}{m^*} \left(\frac{V_0}{W_0} \right)$ for $d = 2$. The discontinuity in G_{diff} is very small when the condition $W_0 \gg V_0$ of observability of transition is satisfied.

ACKNOWLEDGMENTS

We are grateful to the National Science Foundation for supporting the work at Syracuse University through Grant No. DMR92-17284 and DMR94-19257. M.P.A.F. has been supported by grants PHY94-07194, DMR-9400142 and DMR95-28578. L.-WC and MCM thank Alan Middleton for many illuminating discussions.

APPENDIX A: SINGLE FLUX LINE AND ONE COLUMNAR DEFECT

In order to gain some understanding of the dependence of our results on the size L_x of the system in the direction of the external driving force (or tilt field for the magnetic flux line), it is instructive to consider the action of a transverse tilt field on a flux line pinned by a *single* attractive columnar defect. The partition function is given by Eq. (3.4), with $U(\mathbf{r})$ the pinning potential due to the single impurity, chosen for simplicity as an attractive δ -function,

$$U(\mathbf{r}) = -U_0\delta(\mathbf{r}). \quad (\text{A1})$$

Following Ref. [17], Eq. (3.4) can be thought of as a path integral in imaginary time and the partition function can be rewritten as a quantum mechanical matrix element,

$$Z(\mathbf{r}_\perp, \mathbf{0}; L) = \langle \mathbf{r}_\perp | e^{-L\mathcal{H}/T} | \mathbf{0} \rangle, \quad (\text{A2})$$

where $|\mathbf{0}\rangle$ and $\langle \mathbf{r}_\perp|$ are initial and final states localized at $\mathbf{0}$ and \mathbf{r}_\perp , respectively, and the ‘‘Hamiltonian’’ \mathcal{H} is the operator,

$$\mathcal{H} = -\frac{1}{2\tilde{\epsilon}_1}(T\nabla - \mathbf{h})^2 + U(\mathbf{r}). \quad (\text{A3})$$

The operator \mathcal{H} is nonhermitian as $\mathcal{H}^\dagger(h) = \mathcal{H}(-h)$. To find its spectrum we need to solve both the right and left eigenvalue problem, defined by,

$$\mathcal{H}u_n^R = E_n u_n^R, \quad (\text{A4})$$

and

$$\mathcal{H}^\dagger u_n^L = E_n u_n^L, \quad (\text{A5})$$

where $u_n^R(x)$ and $u_n^L(x)$ are the right and left eigenfunction, respectively, normalized according to $\int_0^L dx u_n^L(x) u_n^R(x) = 1$, and E_n are the corresponding eigenvalues. The path integral (3.4) can then be expressed in terms of the eigenvalues and eigenfunctions of the fictitious quantum problem, as

$$Z(\mathbf{r}_\perp, \mathbf{0}; L) = \sum_n u_n^R(\mathbf{r}_\perp) u_n^L(\mathbf{0}) e^{-E_n L/T}. \quad (\text{A6})$$

This is also equivalent to writing the path integral in terms of the eigenvalues of a corresponding transfer matrix. In the limit $L \rightarrow \infty$ the smallest eigenvalue dominates and the free energy per unit length $g(h)$ of the flux line is determined by the real part of the ground state energy E_0 of the quantum problem, according to $g(h) = E_0 + h^2/2\tilde{\epsilon}_1$. For localized states, the ground state wavefunction $u_0(\mathbf{r})$ determines the localization length of the flux line [17].

For simplicity we begin by considering a flux line in $1+1$ dimensions, with x the direction of the applied tilt field. The vortex free energy is given by the ground state of the non-hermitian ‘‘Schrödinger equation’’, given by [18],

$$\left[-\frac{1}{2\tilde{\epsilon}_1} \left(T \frac{d}{dx} - h \right)^2 - U_0 \delta(x) \right] u(x) = E u(x), \quad (\text{A7})$$

to be solved with periodic boundary conditions, $u(0) = u(L_x)$. We are considering here the right eigenvalue problem and dropping for simplicity of notation the labels on the eigenfunction. The solutions of Eq. (A7) for $x \neq 0$ are given by $u_\pm(x) = e^{\pm\kappa x} e^{hx/T}$, with $\kappa = \sqrt{-2\tilde{\epsilon}_1 E/T^2}$. The general solution of Eq. (A7) can then be written as

$$u(x) = A e^{(h/T+\kappa)x} + B e^{(h/T-\kappa)x}, \quad (\text{A8})$$

where A and B are constants to be determined by the periodic boundary condition and the condition that the wavefunction has a slope discontinuity determined by the δ -function, $\left(\frac{du}{dx}\right)_{L_x} - \left(\frac{du}{dx}\right)_0 = \frac{2\tilde{\epsilon}_1 U_0}{T^2} u(0)$. The condition for a nontrivial solution to exist yields the eigenvalue equation, given by,

$$\cosh(hL_x/T) - \cosh(\kappa L_x) + \frac{\tilde{\epsilon}_1 U_0}{T^2 \kappa} \sinh(\kappa L_x) = 0. \quad (\text{A9})$$

In the limit $L_x \rightarrow \infty$, there is one localized ground state for $h < h_c$, with $h_c = \tilde{\epsilon}_1 U_0/T$. For $h \geq h_c$ all states are extended. The ground state energy is given by,

$$E_0^\infty = -\frac{h_c^2}{2\tilde{\epsilon}_1}, \quad h < h_c$$

$$E_0^\infty = -\frac{h^2}{2\tilde{\epsilon}_1}, \quad h \geq h_c, \quad (\text{A10})$$

The ground state wavefunction is given by

$$u_0^R(x) = \sqrt{\frac{T}{h_c}} e^{-\frac{(h_c-h)x}{T}} \quad h < h_c$$

$$u_0^R(x) = \frac{1}{\sqrt{L_x}}, \quad h \geq h_c. \quad (\text{A11})$$

It is exponentially localized for $h < h_c$, with localization length $\xi \sim \frac{T}{(h_c-h)}$. If the system is infinitely long in the field(z -) direction ($L \rightarrow \infty$), the flux line free energy per

unit length is simply $g(h) = E_0 + h^2/2\tilde{\epsilon}_1$. The free energy per unit length is shown in Fig.5 as a function of h (thick line). Clearly the magnetization m_\perp is $m_\perp = -h/\tilde{\epsilon}_1$ below h_c and cancels the applied field, yielding $b_\perp = 0$, as required for transverse Meissner effect. For $h \geq h_c$, $b_\perp = h/\tilde{\epsilon}_1$, which is the value in the absence of disorder. The induction has a jump discontinuity at h_c .

We now discuss the corrections to the above results due to a finite system size L_x . This will be useful for understanding our numerical results for the driven CDW. One can study analytically the finite size corrections in the limit $L_x h \gg 1$. Keeping the leading finite size correction, the real part of the ground state energy is given by

$$\begin{aligned}
 E_0(L_x) &\approx -\frac{h_c^2}{2\tilde{\epsilon}_1} \left[1 + 2e^{-L_x(h_c-h)/T} \right], & h < h_c \\
 E_0(L_x) &\approx -\frac{h^2}{2\tilde{\epsilon}_1} + \frac{1}{L_x} \left(\frac{hT}{\tilde{\epsilon}_1} \right) \ln \left(1 - \frac{h_c}{h} \right) \\
 &\approx -\frac{h^2}{2\tilde{\epsilon}_1} - \frac{Th_c}{L_x \tilde{\epsilon}_1}, & h \geq h_c, \quad (\text{A12})
 \end{aligned}$$

where we have assumed $h \gg h_c$. In the region $h < h_c$, where the flux line is pinned on the defect, the finite size corrections vanish exponentially as $\frac{L_x}{\xi}$, with ξ the localization length. For $h > h_c$ the flux line is depinned and samples the whole sample. In this region the asymptotic ($h \gg h_c$) correction to the ground state energy of an infinite system vanishes only as $\frac{1}{L_x}$. The free energy $g(h, L_x)$ is shown in Fig. 5 for a few values of system size L_x .

The CDW frequency shift δv_{sing} is simply proportional to the negative of $g(h)$ (see table 1). The similarity in the finite size dependence of Figs. 1 and 5 is apparent. Finally, Fig. 6 shows the dependence of the normalized probability density in the ground state $P(x) = u^R(x)u^L(x)$ on system size L_x . The tilt induces a mismatch of order $e^{-(h_c-h)L_x/T}$ in the wavefunction at the system boundaries. For $h \ll h_c$ this mismatch is exponentially small and the periodic boundary conditions are easily accommodated. For $h \sim h_c$ the boundary conditions force a large negative gradient in the wave function, as apparent from Fig. 6. Physically this corresponds to the fact that for $h \sim h_c$ and finite L_x long sections of the flux line are still pinned on a strong columnar pin, yielding large finite size effect in the region above the depinning transition.

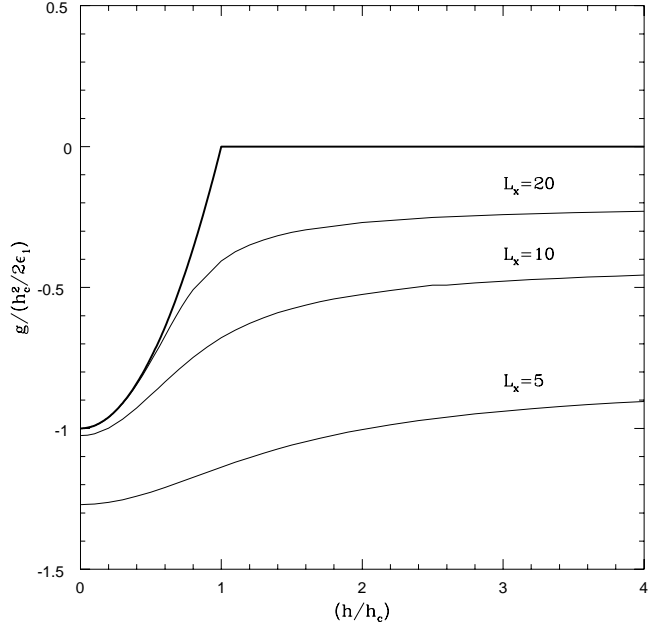


Fig.5

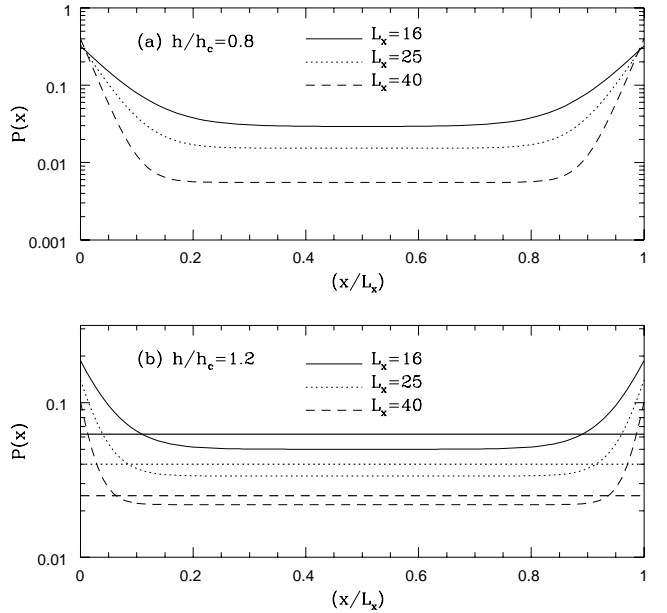


Fig.6

[1] G. Gruner, Rev. Mod. Phys. **60**, 1129(1988).

- [2] D. S. Fisher, M. P. A. Fisher, D. Huse, Phys. Rev. **B43**, 130(1991).
- [3] P. Sibani and P. B. Littlewood, Phys. Rev. Lett. **64**, 1305(1990). 1336(1991).
- [4] O. Narayan and D. S. Fisher, Phys. Rev. **B 46**, 11520(1992). **263**, 943(1994).
- [5] A. E. Koshelev and V. M. Vinokur, Phys. Rev. Lett. **73**, 3580(1994).
- [6] L. Balents and M. P. A. Fisher, Phys. Rev. Lett. **75**, 4270(1995).
- [7] L. Sneddon, M. C. Cross and D. S. Fisher, Phys. Rev. Lett. **49**, 292(1982).
- [8] L.-W. Chen, L. Balents, M. P. A. Fisher, and M. C. Marchetti, unpublished.
- [9] M. Kardar, G. Parisi, and Y. C. Zhang, Phys. Rev. Lett **56**, 889(1986).
- [10] H. Fukuyama and P. A. Rice, Phys. Rev. **B17**, 535(1978).
- [11] J. Krug, Phys. Rev. Lett **75**, 1795(1995).
- [12] M. Rost and H. Spohn, Phys. rev. **E49**, 3709(1994).
- [13] J. G. Amar, P.-M. Lam, and F. Family, Phys. Rev. **E47**, 3242(1993).
- [14] D. Ertas and M. Kardar, Phys. Rev. **E48**, 1228(1993).
- [15] L. Balents, S. H. Simon, Phys. Rev. **B51**, 6515(1995).
- [16] N. Hatano and D. R. Nelson, cond-mat/9603165.
- [17] See, for example, D. R. Nelson in *Phenomenology and Applications of High Temperature Superconductors: the Los Alamos Symposium, 1991*, (Addison-Wesley, Mass. 1992).
- [18] As discussed in Ref. [16], the eigenvalues of the non-hermitian operator \mathcal{H} are in general complex. Here we discuss in detail only the real part of the ground state eigenvalue which determines the flux line free energy. The ground state eigenvalue is real for $L_x \rightarrow \infty$, but acquires a nonzero imaginary part at finite L_x for $h > h_c$.

Figure Captions

Fig. 1 The singular part δv_{sing} of the CDW velocity as a function of applied force σ for various system sizes. The critical force σ_c is estimated to be $\sigma_c \sim \sqrt{2\lambda_0 F_0} = \sqrt{2}$ for the set of parameters used in the figure.

Fig. 2 The derivative of the CDW velocity $\langle \partial_t \phi \rangle$ with respect to the applied forces σ . This figure can also be interpreted as the transverse magnetization m (measured in units of $\frac{\phi_0}{4\pi}$) versus transverse magnetic field H_x for a flux line in columnar defects.

Fig. 3 Two-dimensional CDW phase configurations $\phi(x, y; t) - \overline{\phi(x, y; t)}$ for various driving forces σ at long time for $\lambda_0 = 1.0$ and $F_0 = 1.0$. The estimated σ_c is $\sigma_c = \sqrt{2}$. The contour plots are (a) $\sigma = 0.1$, (b) $\sigma = 1.4$ and (c) $\sigma = 10.0$. The relative value of the CDW phase ϕ is given by the greyscale intensity, with the bright-

est spots corresponding to the highest ϕ and the darkest spots the lowest ϕ .

Fig. 4 The figure shows the scaling collapse of the interface width $w(L_x, L_\perp)$ according to the ansatz Eq. (4.2) for $d = 2$. The parameter values are indicated and $\sigma = 50.0$.

Fig. 5 The free energy per unit length $g(h)$ of a tilted flux line pinned by a single defect as a function of $\frac{h}{\epsilon_1}$. Both the result in the thermodynamic limit $L_x \rightarrow \infty$ (thick line) and the finite size results are shown.

Fig. 6 Probability density $P(x) = u^R(x)u^L(x)$ for various system sizes at (a) $h = 0.8h_c$ and (b) $h = 1.2h_c$. In Fig. (a) the probability density decays exponentially to zero over a length $x \sim \xi \sim 5$ in the limit $L_x \rightarrow \infty$. The finite-size correction are determined by the value of $P(x)$ in the central flat region. They are therefore rather small even for not too large a value of L_x . In Fig. (b) $P(x) = \frac{1}{L_x}$ in the limit $L_x \rightarrow \infty$. This value is shown as an horizontal line for each L_x .

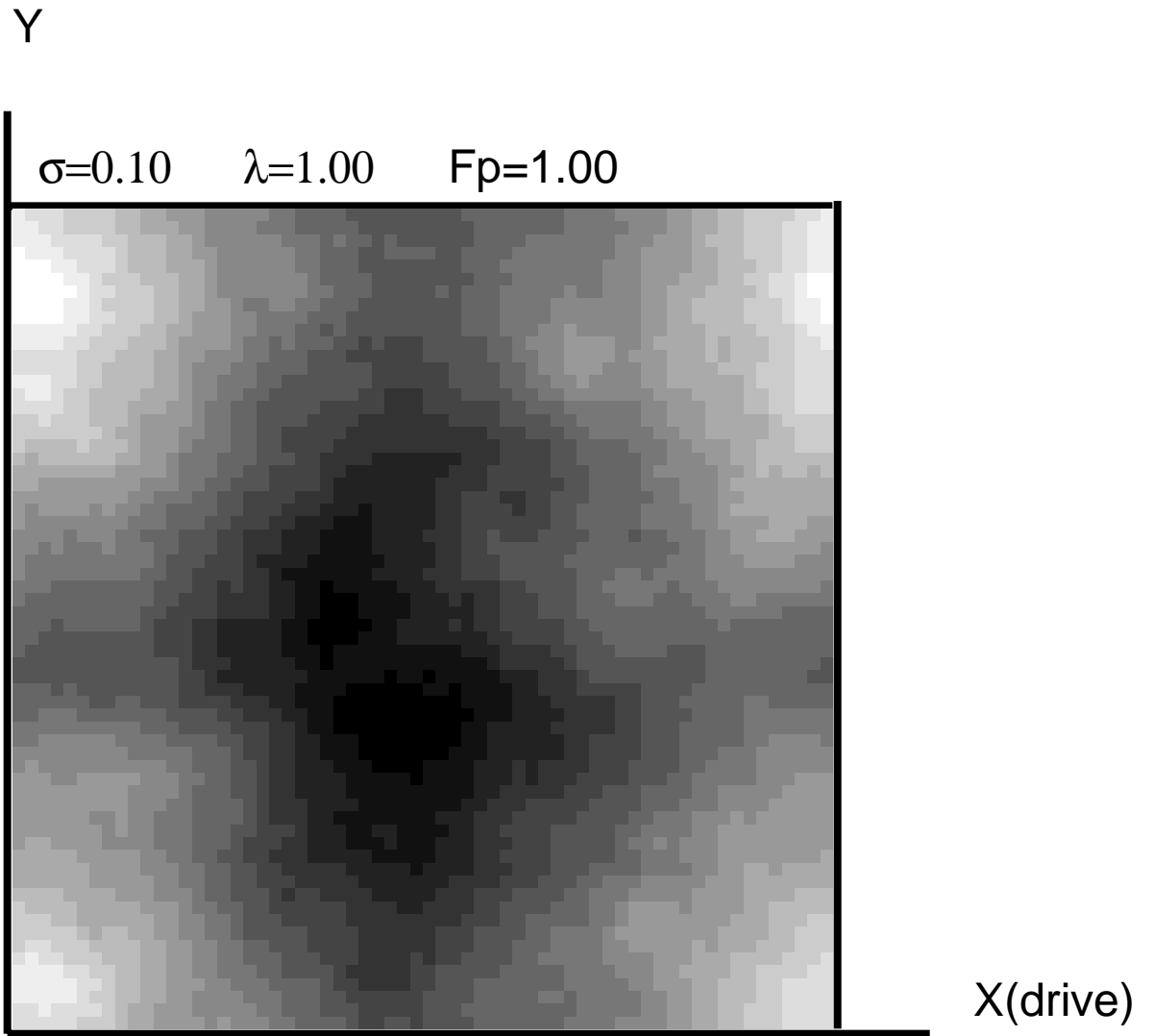


Fig. 3(a)

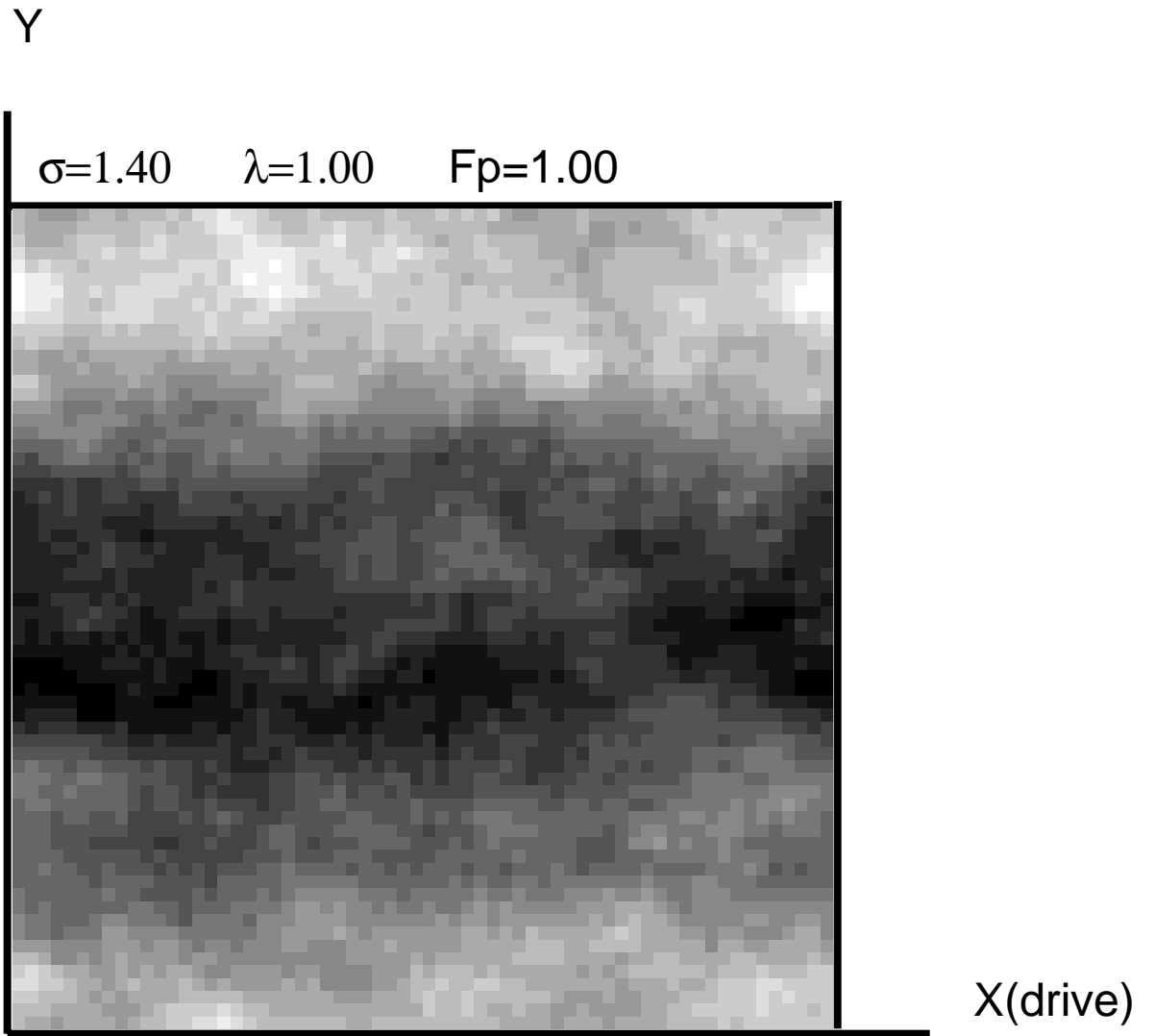


Fig. 3(b)

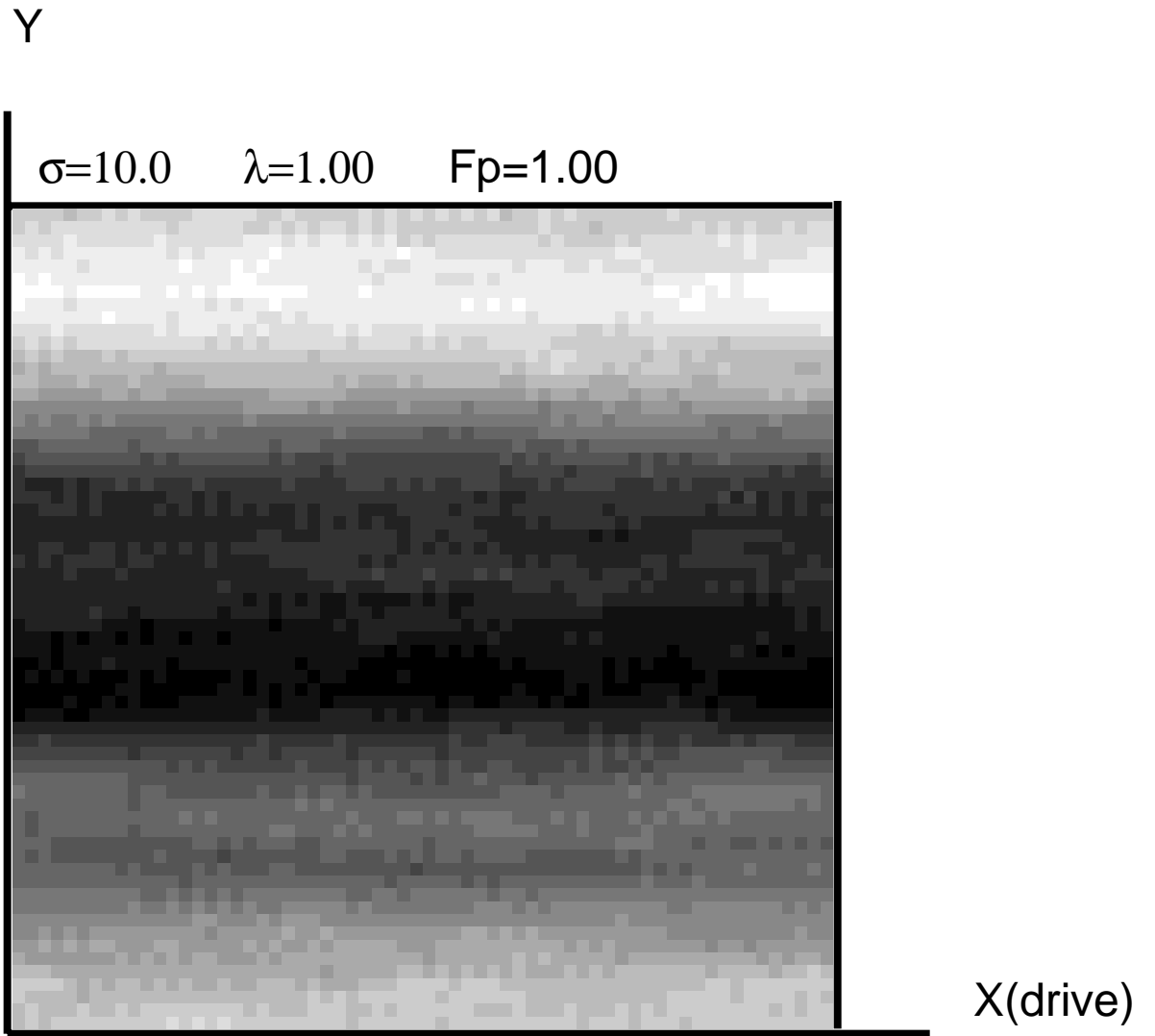


Fig. 3(c)